

## Taichi: Signal Dodging and Interference Guiding to Enhance Data Transmission

LIYUAN XIAO<sup>1</sup>, ZHAO LI<sup>2</sup>, LU ZHEN<sup>2</sup>, JIA LIU<sup>3</sup> AND YANG XU<sup>4</sup>

<sup>1</sup>*School of Information Science and Technology*

*Northwest University*

*Xi'an, Shaanxi, 710127 P.R. China*

*E-mail: simple\_xly@126.com*

<sup>2</sup>*School of Cyber Engineering*

<sup>4</sup>*School of Economics and Management*

*Xidian University*

*Xi'an, Shaanxi, 710126 P.R. China*

*E-mail: {zli; yxu}@xidian.edu.cn; luzhen0320@gmail.com*

<sup>3</sup>*Center for Cybersecurity Research and Development*

*National Institute of Informatics*

*Chiyoda-ku, Tokyo 101-8430, Japan*

*E-mail: jliu871219@gmail.com*

With the rapid development of wireless technologies, interference has become a main impediment to network performance, making interference management (IM) a critical issue that warrants a thorough investigation. In this paper, we propose a novel IM technique, called *signal dodging and interference guiding* (SDIG). With this method, we first intellectually move the data transmission away from the interference, which we call *signal dodging*, hence can partially avoid the influence of disturbance to the desired signal. Then, we employ existing IM method, including zero-forcing (ZF) reception, interference alignment (IA), interference steering (IS), *etc.*, to further eliminate the impact of interference on the interfered receiver (Rx) via nullifying the disturbance (using ZF) or *guiding/adjusting* the interference to be orthogonal to the desired transmission (with IA, IS, *etc.*). The SDIG consists of two-phase processing, the first one is modifying the desired signal, and the second one is mitigating the interference. This is similar to the idea of Taichi in that both involve the actions of passive defense and active attack. Therefore, we also use the term *Taichi* as an equivalent for SDIG. Our in-depth analysis and simulation have shown that with the proposed scheme, the spatial domain communication resource of the interfered transmission-pair can be properly and efficiently utilized, thus both the interfered user's and the system's spectral efficiency (SE) can be significantly improved.

**Keywords:** interference management, heterogeneous networks, signal dodging, interference guiding, spectral efficiency

### 1. INTRODUCTION

With the tremendous growing of subscribers' communication demand [1], the capacity of traditional cellular systems needs to be substantially improved in the 5G era. Network densification, *i.e.*, deploying small cells on top of existing cellular networks to increase the frequency reuse, has been widely accepted by the operators as a promising solution for enhancing network capacity [1]. However, as the degree of frequency reuse increases, interference has become the key impediment in further improving the network performance.

Received August 19, 2019; revised November 19, 2019; accepted December 5, 2019.

Communicated by Xiaohong Jiang.

Therefore, effective interference management (IM) is regarded as critical issue that warrants thorough investigation.

IM is a fundamental issue in wireless communications. Existing IM methods in cellular networks [2, 3] employ resource partition to isolate mutually interfering transmissions, *e.g.*, time division multiplexing (TDM) and frequency division multiplexing (FDM), so that interference can be effectively mitigated. However, these mechanisms may cause degradation of frequency efficiency due to under-utilization of spectrum. Besides, there have been various signal processing techniques that can also be adopted for IM, such as zero-forcing (ZF) reception [4], zero-forcing beamforming (ZFBE) [5], interference alignment (IA) [6, 7], interference neutralization (IN) [8] and interference steering (IS) [9]. However, none of these existing IM methods are free of cost. That is, all IM methods manage interference at the cost of consuming certain types of communication resources (the details can be found in the related work part).

As is known, the realization of data transmission relies on the consumption of certain types of resources such as time, frequency, code, space and power. The first three types have been adopted in some practical systems, *e.g.*, advanced mobile phone service (AMPS), global system for mobile communications (GSM) and code division multiple access (CDMA) systems. Besides, there have been numerous research works on the utilization of spatial domain resource such as MIMO, Massive MIMO, Small cell and device-to-device (D2D), and power domain resource, *e.g.*, non-orthogonal multiple access (NOMA), so that the system's capacity can be further improved.

Based on the above discussion, given limited communication resource, the more resources used for IM, the less available for the data transmission. In the design of IM methods, some researchers put emphasis on the effectiveness of interference suppression or elimination, while the others focus on the intelligent allocation of resources to multiple interfering data transmissions. However, joint design of the above two aspects is left unaddressed. How to appropriately allocate resources to data transmission and IM so as to optimize the system's spectral efficiency (SE) is an important issue that is worthy of a thorough investigation.

Since MIMO can enhance system's SE and realize IM by exploiting spatial resource, we will present our design in a MIMO scenario. In a conventional MIMO transmission, the principal eigenmode has the largest channel gain, thus beamforming (BF) employs this best eigenmode for data transmission. However, in practice, the impact of interference on the desired transmission in the principal eigenmode may be strong, *i.e.*, the projection of interference on the principal eigenmode is large. In such a case, it may be unwise to select the principal eigenmode for the desired signal's transmission. Motivated by this observation, we present a novel *signal dodging and interference guiding* (SDIG) scheme in this paper. By properly selecting eigenmode for data transmission and adjusting the interference's spatial feature based on the strength of interference, spatial features of interference and eigenmode occupied by the desired data transmission, users' SE can be improved. The proposed method consists of two phases, *i.e.*, signal dodging (SD) and interference guiding (IG). The first phase aims at choosing an eigenmode suffering less interference in data transmission, which is characterized by passive interference management (PIM). As a comparison, ZF reception, ZFBE, IS and IA are featured as active IM (AIM) since these schemes are realized by either suppressing or modifying the interfering signal actively. The second phase of SDIG, *i.e.*, IG, focuses on employing proper AIM method to further

reduce the influence of disturbance. Therefore, the proposed mechanism incorporates both interference suppression and data transmission, hence showing advantages over those schemes considering only one aspect. Since the idea of SDIG is similar to that of Taichi, *i.e.*, dodging the attack from an opponent and making the opponent away by exploiting the opponent's own feature, we also adopt this term as the name of our method. In this paper, we consider the downlink transmission in heterogeneous networks (HetNets) consisting of overlapping macro- and pico-cell sharing the same frequency band. By taking into consideration of the practical factors such as the path loss and the transmit power difference between the base stations (BSs), we propose SDIG/Taichi to improve the users' SE performance.

The contributions of this paper are two-fold:

- Proposal of signal dodging (SD). We derive the criterion of whether to adopt SD or not, according to the strength of interference and the spatial correlation of the desired signal and interference.
- Effective utilization of PIM and AIM. To be specific, by employing interference guiding (IG) after SD, SDIG/Taichi is realized. With SDIG/Taichi, resources are appropriately allocated to the desired signal's transmission and IM, yielding improved system's SE.

The rest of this paper is organized as follows. Section 2 presents some related works, while Section 3 describes the system model. Section 4 designs SD and discusses its necessity, and Section 5 presents SDIG/Taichi for effective utilization of communication resources. Section 6 discusses the generalization of the proposed mechanism, and Section 7 evaluates the performance of SDIG/Taichi. Finally, Section 8 concludes the paper.

Throughout this paper, we use the following notations. The set of complex numbers is denoted by  $\mathbb{C}$ , while vectors and matrices are represented by bold letters, respectively. Let  $\mathbf{X}^H$  and  $\mathbf{X}^{-1}$  denote the Hermitian and inverse of matrix  $\mathbf{X}$ .  $\|\cdot\|$  indicates the Euclidean norm.  $E(\cdot)$  denotes statistical expectation.  $\langle \mathbf{a}, \mathbf{b} \rangle$  represents the inner product of two vectors.

## 2. RELATED WORK

Among those IM methods mentioned in the introduction part, ZF reception eliminates the impact of interference on the desired signal by employing a filter vector orthogonal to the disturbance at the interfered receiver (Rx) [4]. ZFBF appropriately adjusts the transmitted beams so that the spatial feature of the interfering signals can be orthogonal to that of the desired signal at the interfered Rx [5]. IA aims at constructing signals at the interfering transmitters (Tx) so that these signals overlap with each other (*i.e.*, aligning in a compressed subspace) at their undesired Rx, hence the degree of freedoms (DoFs)<sup>1</sup> for desired data transmission is maximized [6, 7]. With IN, a neutralizing signal of the same strength and opposite direction with respect to (w.r.t.) the interference is generated, so that the interfering signal at the undesired destination can be mitigated over the air, leading to the interference-free transmission from a source to its destination [8]. By making use of

<sup>1</sup> DoF is defined as the first-order approximation of sum rate capacity at high signal-to-noise ratio (SNR) regime [10, 11]. In point to point multiple-input multiple-output (MIMO) case, DoF can be regarded as the number of spatially decoupled parallel channels obtained by applying singular value decomposition (SVD) to the channel matrix [12]. In this paper, we use DoF to denote the number of concurrent interference-free data transmissions that the system can support. We also use DoF to represent the spatial subchannel that can be used for data transmission.

interference at the interfered Rx is orthogonal to its intended signal [9].

However, none of the abovementioned IM methods are free of cost. By shaping transmitted beam, both ZFBF and IA incur the loss of the adjusted signal's strength. ZF reception yields the desired signal's power loss while eliminating the influence of disturbance. Moreover, ZFBF and ZF reception require multiple antennas at the Tx and Rx, respectively, whereas for IA, both ends of the communication link should be equipped with multiple antennas [13]. With IN, since interference is neutralized over the air, no extra DoF for IM is required, but generating neutralizing signal consumes transmit power at the Tx associated with the interfered Rx [13]. As for IS, one DoF at the interfered Rx is required to accommodate the adjusted disturbance which is similar to IA; and moreover, generating steering signal incurs transmit power overhead like IN. From the above discussion, we can conclude that IM consumes some types of communication resources such as DoF and power. However, such resources can also be used for the desired data transmission. Therefore, IM is crucial to the improvement of data transmission in two aspects, *i.e.*, interference suppression/mitigation and communication resources consumption.

### 3. SYSTEM MODEL

We consider downlink communication in a hybrid cellular system consisting of overlapping macro- and pico-cells. Macro user equipment (MUE) and pico user equipment (PUE) are served by macro base station (MBS) and pico base station (PBS), respectively. MBS and PBS are equipped with  $N_{T_1}$  and  $N_{T_0}$  antennas while MUE and PUE have  $N_{R_1}$  and  $N_{R_0}$  antennas. Let  $P_{T_1}$  and  $P_{T_0}$  be the transmit power of MBS and PBS, respectively. The picocell operates in an open mode and allows the users within its coverage to access it. Since the downlink transmissions in macro- and pico-cell share the same frequency band, there is interference between them. However, as PBS's transmit power is small and MUE is not within its coverage, interference from PBS to MUE can be omitted. Although PUE can be anywhere within the picocell, we take the worst case as an example, *i.e.*, PUE is at the edge of the picocell. Therefore, PUE receives the weakest desired signal.

To achieve as high SE as possible, the transmission from MBS to MUE is realized based on their own CSI, which is the same as the case of point-to-point (p2p) MIMO. So, we only study the management of interference from MBS to PUE. Let  $\mathbf{h}_1 \in \mathbb{C}^{N_{R_1} \times N_{T_1}}$  be the channel matrix from MBS to MUE. The channel matrices from PBS and MBS to PUE are represented by  $\mathbf{h}_0 \in \mathbb{C}^{N_{R_0} \times N_{T_0}}$  and  $\mathbf{h}_{10} \in \mathbb{C}^{N_{R_0} \times N_{T_1}}$ , respectively. A spatially uncorrelated Rayleigh flat fading channel model is assumed so that the elements of these channel matrices are modeled as independent and identically distributed zero-mean unit variance complex Gaussian random variables. All UEs experience block fading, *i.e.*, channel parameters in a block consisting of several successive transmission cycles remain constant in the block and vary randomly between blocks. The BSs operate in a synchronized slot structure. In each time slot, each BS allocates different resource block to its UEs [14], so that co-channel interference (CCI) within a cell is avoided. The BSs can acquire CSI accurately via UEs' feedback, and share UEs' data information or/and CSI with other BSs via X2 interface [15]. We assume the backhaul dedicated to CSI and data information sharing, and signaling delivery is error free, and with the latency at a negligible level relative to the time scale on which the channel state varies.

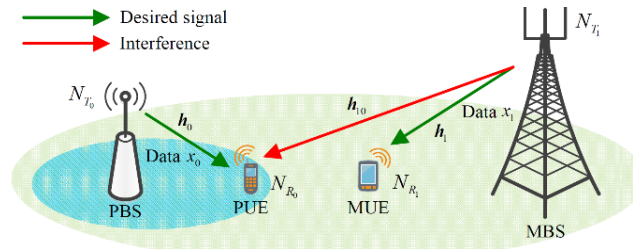


Fig. 1. System model.

For clarity of exposition, we begin our design from  $N_{T_1} = N_{T_0} = N_{R_1} = N_{R_0} = 2$ . We assume BF is employed for each downlink transmission. Desired data symbols transmitted from MBS and PBS to MUE and PUE are denoted by  $x_1^{(1)}$  and  $x_0^{(1)}$ , respectively, satisfying  $E(\|x_1^{(1)}\|^2) = E(\|x_0^{(1)}\|^2) = 1$ . The path loss from MBS and PBS to a UE is modeled as  $L_{(\cdot)} = 128.1 + 37.6 \log_{10}[\rho_{(\cdot)}/10^3]$  dB and  $L_{(\cdot)} = 38 + 30 \log_{10}[\rho_{(\cdot)}]$  dB [16], where the variable  $\rho_{(\cdot)}$ , measured in meters (m), is the distance from the Tx to the Rx.

#### 4. DESIGN OF SIGNAL DODGING

In this section, we will give the design of signal dodging. Before delving into details, we first present basic signal processing of the pico and macro transmissions. The received signal at PUE is expressed as:

$$\mathbf{y}_0 = \sqrt{P_{T_0}^e} 10^{-0.05L_0} \mathbf{h}_0 \mathbf{p}_0^{(1)} x_0^{(1)} + \sqrt{P_{T_1}^e} 10^{-0.05L_{i_0}} \mathbf{h}_{i_0} \mathbf{p}_1^{(1)} x_1^{(1)} + \mathbf{z}_0 \quad (1)$$

where the column vectors  $\mathbf{p}_0^{(1)}$  and  $\mathbf{p}_1^{(1)}$  are the precoders for data symbols  $x_0^{(1)}$  and  $x_1^{(1)}$  at PBS and MBS, respectively. The first and second terms on the right hand side (RHS) of Eq. (1) are the desired signal from PBS and the interference from MBS. We employ singular value decomposition (SVD) based precoding and receive filtering as an example. Applying SVD to  $\mathbf{h}_1$ , we have  $\mathbf{h}_1 = \mathbf{U}_1 \mathbf{D}_1 \mathbf{V}_1^H$ . We adopt  $\mathbf{p}_1^{(1)} = \mathbf{v}_1^{(1)}$  where  $\mathbf{v}_1^{(1)}$  is the first column of the right singular matrix  $\mathbf{V}_1$ , corresponding to the principal eigenmode of  $\mathbf{h}_1$ .  $\mathbf{z}_0$  is an additive white Gaussian noise (AWGN) vector whose elements have zero-mean and variance  $\sigma_n^2$ . For clarity of exposition, we define  $P_{T_0}^e = P_{T_0} 10^{-0.1L_0}$  and  $P_{T_1}^e = P_{T_1} 10^{-0.1L_{i_0}}$  where  $P_{T_0}^e$  and  $P_{T_1}^e$  indicate the transmit power of PBS and MBS incorporated with path loss perceived by PUE, respectively.

The estimated signal at PUE after post-processing with receive filter  $\mathbf{f}_0^{(1)}$  is:

$$\bar{\mathbf{y}}_0 = \sqrt{P_{T_0}^e} [\mathbf{f}_0^{(1)}]^H \mathbf{h}_0 \mathbf{p}_0^{(1)} x_0^{(1)} + \sqrt{P_{T_1}^e} [\mathbf{f}_0^{(1)}]^H \mathbf{h}_{i_0} \mathbf{p}_1^{(1)} x_1^{(1)} + [\mathbf{f}_0^{(1)}]^H \mathbf{z}_0. \quad (2)$$

As a counterpart, the received signal at MUE is:

$$\mathbf{y}_1 = \sqrt{P_{T_1}^e} 10^{-0.05L_1} \mathbf{h}_1 \mathbf{p}_1^{(1)} x_1^{(1)} + \mathbf{z}_1. \quad (3)$$

The estimated signal at MUE employing  $\mathbf{f}_1^{(1)}$  as the filter is obtained as:

$$\bar{y}_1 = \sqrt{P_T^e} 10^{-0.05L_1} [\mathbf{f}_1^{(1)}]^H \mathbf{h}_1 \mathbf{p}_1^{(1)} x_1^{(1)} + [\mathbf{f}_1^{(1)}]^H \mathbf{z}_1. \quad (4)$$

In the following discussion, if MBS doesn't adjust its transmission, we can without loss of generality employ  $\mathbf{f}_1^{(1)} = \mathbf{u}_1^{(1)}$  where  $\mathbf{u}_1^{(1)}$  is the principal right singular vector of  $\mathbf{h}_1$ .

As is known, in most existing transmission schemes, the principal eigenmode is usually used for the desired signal's transmission due to its high channel gain. However, when interference highly correlates with the principal eigenmode, it would be unwise to keep the desired transmission in the severely polluted principal eigenmode. So, we design *signal dodging* (SD) in this section. The main idea of SD is abandoning the severely disturbed eigenmode and adopting the slightly polluted one for the desired transmission, even though the latter has small channel gain. In what follows, we will discuss the necessity of SD.

Eq. (1) can be rewritten as:

$$\mathbf{y}_0 = \sqrt{P_{T_0}^e} \mathbf{h}_0 \mathbf{p}_0^{(1)} x_0^{(1)} + \sqrt{P_{T_1}^e} \mathbf{h}_{10} \mathbf{p}_1^{(1)} x_1^{(1)} + \mathbf{z}_0. \quad (5)$$

The spatial features of the two terms on the RHS of Eq. (5) are determined by the precoding vectors and channel matrices corporately. Applying SVD to  $\mathbf{h}_0$ , we can have  $\mathbf{h}_0 = \mathbf{U}_0 \mathbf{D}_0 \mathbf{V}_0^H$ . Let  $\mathbf{v}_0^{(i)}$  be the  $i^{\text{th}}$  ( $i = 1, 2, \dots, \min(N_{R_0}, N_{T_0})$ ) column vector of  $\mathbf{V}_0$ . We employ two unit vectors, *i.e.*,  $\mathbf{d}_0^{(1)} = \mathbf{h}_0 \mathbf{v}_0^{(1)} / \|\mathbf{h}_0 \mathbf{v}_0^{(1)}\|$  and  $\mathbf{d}_0^{(2)} = \mathbf{h}_0 \mathbf{v}_0^{(2)} / \|\mathbf{h}_0 \mathbf{v}_0^{(2)}\|$ , to represent the spatial features of the eigenmodes of  $\mathbf{h}_0$ . Similarly, the interference's feature is expressed by a unit vector  $\mathbf{d}_x = \mathbf{h}_{10} \mathbf{p}_1^{(1)} / \|\mathbf{h}_{10} \mathbf{p}_1^{(1)}\|$ .

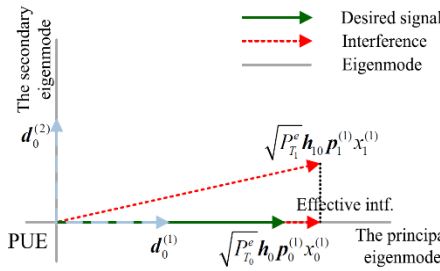


Fig. 2. An illustration of the spatial features of the received signals at PUE.

Without loss of generality, we adopt matched filtering (MF) at PUE, *i.e.*,  $\mathbf{f}_{0,M}^{(1)} = \mathbf{d}_0^{(1)}$  (see in Fig. 2), which maximizes the received desired signal's power.

We define the cosine of the angle between the desired signal and interference as:

$$\cos \theta = \frac{\|\langle \mathbf{d}_0^{(1)}, \mathbf{d}_x \rangle\|}{\|\mathbf{d}_0^{(1)}\| \|\mathbf{d}_x\|} = \frac{\|[\mathbf{d}_0^{(1)}]^H \mathbf{d}_x\|}{\|\mathbf{d}_0^{(1)}\| \|\mathbf{d}_x\|}, 0 \leq \theta \leq \frac{\pi}{2}. \quad (6)$$

Substituting  $\mathbf{p}_0^{(1)} = \mathbf{v}_0^{(1)}$  and  $\mathbf{f}_0^{(1)} = \mathbf{f}_{0,M}^{(1)}$  into Eq. (2), we can calculate PUE's SE as:

$$r_{0,non-SD}^M = \log_2 \left\{ 1 + \frac{P_{T_0}^e \|\mathbf{E}_0^{(1)}\|^2}{\sigma_n^2 + P_{T_1}^e \|[\mathbf{f}_{0,M}^{(1)}]^H \mathbf{E}_x\|^2} \right\} \quad (7)$$

where  $\mathbf{E}_0^{(1)} = \mathbf{h}_0 \mathbf{v}_0^{(1)}$  and  $\mathbf{E}_x = \mathbf{h}_{10} \mathbf{p}_1^{(1)}$ . The superscript  $M$  in  $r_{0,non-SD}^M$  indicates MF is adopted

by the Rx, while the subscript *non-SD* means that SD is not employed. From Eq. (7) we can see that with MF, the interference component still influences the desired signal. Since  $\|[\mathbf{f}_{0,M}^{(1)}]^H \mathbf{E}_x\|^2 = \|\mathbf{E}_x\|^2 \|[\mathbf{d}_0^{(1)}]^H \mathbf{d}_x\|^2 = \|\mathbf{E}_x\|^2 \cos^2 \theta$  holds, Eq. (7) can be simplified as:

$$r_{0,non-SD}^M = \log_2 \left\{ 1 + \frac{P_{T_0}^e \|\mathbf{E}_0^{(1)}\|^2}{\sigma_n^2 (1 + Z \cos^2 \theta)} \right\} \quad (8)$$

where  $Z = P_{T_1}^e \|\mathbf{E}_x\|^2 / \sigma_n^2$ .

By employing signal dodging, the desired signal is moved from the principal eigenmode to the secondary one, *i.e.*,  $\mathbf{p}_0^{(1)} = \mathbf{v}_0^{(2)}$ . Then, Eq. (8) becomes

$$r_{0,SD}^M = \log_2 \left\{ 1 + \frac{P_{T_0}^e \|\mathbf{E}_0^{(2)}\|^2}{\sigma_n^2 (1 + Z \sin^2 \theta)} \right\} \quad (9)$$

where  $\mathbf{E}_0^{(2)} = \mathbf{h}_0 \mathbf{v}_0^{(2)}$ , indicating the spatial feature of the transmission via the secondary eigenmode of  $\mathbf{h}_0$ .

Next, we will discuss the condition under which SD is applied. Letting  $r_{0,SD}^M > r_{0,non-SD}^M$ , we have:

$$\frac{\|\mathbf{E}_0^{(1)}\|^2 - \|\mathbf{E}_0^{(2)}\|^2}{\|\mathbf{E}_0^{(1)}\|^2 \|\mathbf{E}_0^{(2)}\|^2} < \frac{Z(\cos^2 \theta \|\mathbf{E}_0^{(2)}\|^2 - (1 - \cos^2 \theta) \|\mathbf{E}_0^{(1)}\|^2)}{\|\mathbf{E}_0^{(1)}\|^2 \|\mathbf{E}_0^{(2)}\|^2}. \quad (10)$$

We define the ratio of the amplitude gain of the principal eigenmode to that of the secondary eigenmode as  $\alpha = \|\mathbf{E}_0^{(1)}\|^2 / \|\mathbf{E}_0^{(2)}\|^2$ . Then, Eq. (10) can be simplified as:

$$\cos^2 \theta > \frac{\alpha - 1}{Z(\alpha + 1)} + \frac{\alpha}{\alpha + 1}. \quad (11)$$

As long as the above inequality holds, SD is adopted.

It should be noted that although SD can avoid disturbance to some extent, since the channel gain of the secondary eigenmode is less than that of the primary eigenmode, the dodged desired transmission will be degraded. Therefore, the loss of channel gain is the cost of SD. When the decrease of the impact of interference on the desired transmission outweighs the loss of channel gain with SD, the interfered user's SE can be improved compared to that without SD.

## 5. INCORPORATE DESIGN OF SIGNAL DODGING AND INTERFERENCE GUIDING

According to SD, the desired transmission is moved from the principal eigenmode to the secondary one so as to avoid the impact of interference. However, the interference remains unchanged. Therefore, SD belongs to passive IM (PIM). As a counterpart, some IM methods including ZF reception, IS, IA and ZFBF, are realized by either suppressing (ZF reception) or modifying (*i.e.*, IS, IA and ZFBF) interference, thus can be regarded as active IM (AIM). In existing AIM schemes, the desired transmission always occupies the

principal eigenmode while the secondary one is used for IM. However, such methods haven't taken the benefits and cost of IM into account, thus may incur severe transmission performance loss. Therefore, we propose in this section the interference guiding (IG) to modify the interference to the eigenmode most correlated with its original spatial feature, so that the overhead of IM is minimized. That is, both PIM (SD) and AIM (IG) are incorporated in the design of SDIG/Taichi. Although we employ ZF, IA, IS and ZFBF as examples in the design of SDIG/Taichi, it should be noted that other IM methods can also be adopted in realizing SDIG/Taichi. For space limit, we do not elaborate in this paper.

### 5.1 SDIG With ZF Reception (SD-ZF)

We employ ZF reception at the interfered Rx (PUE). Since the filter vector is orthogonal to the interference's feature, the disturbance is mitigated at PUE. However, some desired signal's power loss is incurred. The traditional ZF reception does not consider the spatial correlation between the interference and the desired signal. The higher the correlation, the severer power loss of the desired signal after ZF filtering. In such situation, we can adopt SD-ZF which abandons the principal eigenmode intelligently and utilizes the secondary one for data transmission. So, the attenuation of the desired signal incurred by ZF filtering can be reduced.

We assume PUE employs ZF filter  $\mathbf{f}_{0,O}^{(1)}$  to recover its desired signal. Here, the subscript  $O$  indicates the orthogonal feature of the filter vector w.r.t. the interference. Then, we can have the following equations:

$$\|[\mathbf{f}_{0,O}^{(1)}]^H \mathbf{E}_0^{(1)}\|^2 = \|\mathbf{E}_0^{(1)}\|^2 \|[\mathbf{f}_{0,O}^{(1)}]^H \mathbf{d}_0^{(1)}\|^2 = \|\mathbf{E}_0^{(1)}\|^2 \sin^2 \theta \quad (12)$$

and

$$\|[\mathbf{f}_{0,O}^{(1)}]^H \mathbf{E}_0^{(2)}\|^2 = \|\mathbf{E}_0^{(2)}\|^2 \|[\mathbf{f}_{0,O}^{(1)}]^H \mathbf{d}_0^{(2)}\|^2 = \|\mathbf{E}_0^{(2)}\|^2 \cos^2 \theta. \quad (13)$$

The post-processed signal at PUE is given by:

$$\bar{y}_0 = \sqrt{P_{T_0}^e} [\mathbf{f}_{0,O}^{(1)}]^H \mathbf{h}_0 \mathbf{p}_0^{(1)} x_0^{(1)} + \sqrt{P_{T_1}^e} [\mathbf{f}_{0,O}^{(1)}]^H \mathbf{h}_{10} \mathbf{p}_1^{(1)} x_1^{(1)} + [\mathbf{f}_{0,O}^{(1)}]^H \mathbf{z}_0 \quad (14)$$

where  $\mathbf{p}_0^{(1)}$  can be either  $\mathbf{v}_0^{(1)}$  (with non-SD) or  $\mathbf{v}_0^{(2)}$  (adopting SD), indicating the eigen mode employed by the PBS-PUE transmission pair. In order to eliminate the second term on the RHS of Eq. (14), we define  $\mathbf{v}_\pi = \mathbf{h}_{10} \mathbf{p}_1^{(1)} / \|\mathbf{h}_{10} \mathbf{p}_1^{(1)}\|$ . Then, we can get  $\mathbf{f}_{0,O}^{(1)} = [\mathbf{u}_0^{(i)} - \mathbf{v}_\pi^H \mathbf{u}_0^{(i)} \mathbf{v}_\pi] / \|\mathbf{u}_0^{(i)} - \mathbf{v}_\pi^H \mathbf{u}_0^{(i)} \mathbf{v}_\pi\|$ . When non-SD is adopted, we employ  $\mathbf{u}_0^{(1)}$  in the calculation of  $\mathbf{f}_{0,O}^{(1)}$ , whereas for the SD,  $\mathbf{u}_0^{(2)}$  is adopted.  $\mathbf{u}_0^{(1)}$  and  $\mathbf{u}_0^{(2)}$  are the right singular vectors obtained from applying SVD to  $\mathbf{h}_0$ .

Then, PUE's SE is computed as:

$$r_{0,(SD-ZF)}^O = \log_2 \left\{ 1 + \frac{P_{T_0}^e \|\mathbf{E}_0^{(i)}\|^2 \cos^2(\frac{\pi}{2}i - \theta)}{\sigma_n^2} \right\}. \quad (15)$$

In Eq. (15),  $i = 1$  indicates non-SD is employed, whereas  $i = 2$  denotes the use of SD.



should be noticed that generating steering signal consumes transmit power at PBS [17, 18]. Although the gain of secondary eigenmode is smaller than that of the principal one, the power cost of steering interference to the principal eigenmode may be less than adjusting disturbance to the secondary mode, as long as the interference is highly correlated with the principal eigenmode.

We let PBS generate the steering signal and send it with the desired signal to the PUE [17, 18]. The filtered received signals at PUE with SD-IS can be expressed as:

$$\begin{aligned} \bar{y}_0 = & \sqrt{P_{T_0}^e - P_{IS_H}^e} [\mathbf{f}_{0,M}^{(1)}]^H \mathbf{h}_0 \mathbf{v}_0^{(2)} x_0^{(1)} + \sqrt{P_{IS_H}^e} [\mathbf{f}_{0,M}^{(1)}]^H \mathbf{h}_0 \mathbf{p}_{IS_H} x_1^{(1)} \\ & + \sqrt{P_{T_1}^e} [\mathbf{f}_{0,M}^{(1)}]^H \mathbf{h}_{10} \mathbf{p}_1 x_1^{(1)} + [\mathbf{f}_{0,M}^{(1)}]^H \mathbf{z}_0 \end{aligned} \quad (17)$$

where  $P_{IS_H}^e = P_{IS_H} 10^{0.1L_0}$  and  $P_{IS_H}$  is the power cost for IS. The second term on the RHS of Eq. (17) denotes the steering signal which adjusts the interference to the principal eigenmode. To realize IS, equation  $\sqrt{P_{IS_H}^e} [\mathbf{f}_{0,M}^{(1)}]^H \mathbf{h}_0 \mathbf{p}_{IS_H} = -\sqrt{P_{T_1}^e} \mathbf{h}_{10} \mathbf{p}_1 \sin \theta$  should hold. The use of  $\mathbf{v}_0^{(2)}$  in the first term on the RHS of Eq. (17) indicates that the desired transmission is via the secondary eigenmode, *i.e.*, SD is employed. Then, PUE's SE is given by Eq. (18) as follows,

$$r_{0,SD-IS}^O = \log_2 \left\{ 1 + \frac{(P_{T_0}^e - P_{IS_H}^e) [\lambda_0^{(2)}]^2}{\sigma_n^2} \right\} \quad (18)$$

where  $\lambda_0^{(2)}$  represents the channel gain of the secondary eigenmode of  $\mathbf{h}_0$ . If SD is not adopted, the interference should be steered to the principal eigenmode by employing a steering signal in terms of parameters  $P_{IS_I}$  and  $\mathbf{p}_{IS_I}$ , which can be obtained via solving equation  $\sqrt{P_{IS_I}^e} [\mathbf{f}_{0,M}^{(1)}]^H \mathbf{h}_0 \mathbf{p}_{IS_I} = -\sqrt{P_{T_1}^e} \mathbf{h}_{10} \mathbf{p}_1 \cos \theta$ .

### 5.3 SDIG with Interference Alignment (SD-IA)

With IA, the interferer designs precoder to modify its transmitted signal which causes disturbance to the other Rx, so that the adjusted signal/interference is orthogonal to the interfered Rx's desired transmission. Compared to ZF reception and IS, IA sacrifices the transmission performance of the interfering user-pair while avoiding disturbance to the interfered Rx. Therefore, we use Fig. 5 to illustrate the realization of SD-IA where both PUE and MUE are taken into consideration.

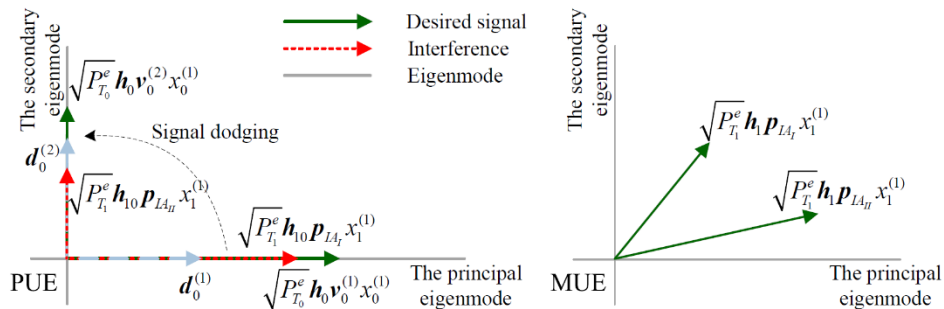


Fig. 5. An illustration of SD-IA.

With SD-IA, the received signal at PUE is:

$$\mathbf{y}_0 = \sqrt{P_0^e} \mathbf{h}_0 \mathbf{v}_0^{(2)} x_0^{(1)} + \sqrt{P_1^e} \mathbf{h}_{10} \mathbf{p}_{1M} x_1^{(1)} + \mathbf{z}_0. \quad (19)$$

$\mathbf{h}_{10} \mathbf{p}_{1M} = \mathbf{h}_0 \mathbf{v}_0^{(1)}$  should hold, indicating the interference from MBS is aligned in the principal eigenmode of  $\mathbf{h}_0$ . The precoder at MBS can be computed as  $\mathbf{p}_{1M} = \mathbf{h}_{10}^{-1} \mathbf{h}_0 \mathbf{v}_0^{(1)}$ . With IA, the received signal at MUE is  $\mathbf{y}_1 = \sqrt{P_1} 10^{-0.05L_d} \mathbf{h}_1 \mathbf{p}_{1M} x_1^{(1)} + \mathbf{z}_1$ . We let PUE adopt  $\mathbf{f}_{0,M}^{(1)} = \mathbf{u}_0^{(2)}$  to recover its desired signal. Then, the estimated signal at PUE is  $\bar{y}_0 = [\mathbf{u}_0^{(2)}]^H \mathbf{y}_0$ . Since the interference component is orthogonal to the desired signal, the second term on the RHS of Eq. (19) becomes zero after post-processing with  $\mathbf{u}_0^{(2)}$ . As for MUE, it can adopt  $\mathbf{f}_{1,M}^{(1)} = \mathbf{h}_1 \mathbf{p}_{1M} / \|\mathbf{h}_1 \mathbf{p}_{1M}\|$  as the receive filter, then we can get  $\bar{y}_1 = [\mathbf{f}_{1,M}^{(1)}]^H \mathbf{y}_1$ .

### 5.4 SDIG With Zero-Forcing Beamforming (SD-ZFBF)

With ZFBF, the Tx related to the interfered Rx, *i.e.*, PBS, designs precoder to preprocess its data, so that the desired transmission is orthogonal to the interference perceived by the interfered PUE. Here it should be noted that in our design, we realize ZFBF at the interfered PBS instead of the interfering Tx, *i.e.*, MBS [5, 8]. Fig. 6 plots the principle of SD-ZFBF. As the figure shows, the adjusted pico-user's transmission is orthogonal to the interference, but locates neither in the principal nor the secondary eigenmode. In a sense, ZFBF implicitly reflects the idea of signal dodging in its precoder design.

By designing  $\mathbf{p}_0^{(1)}$ , the spatial feature of the desired signal of PUE, *i.e.*,  $\mathbf{h}_0 \mathbf{p}_0^{(1)}$ , should be orthogonal to that of the interference, *i.e.*,  $\mathbf{h}_{10} \mathbf{p}_1^{(1)}$ . Then, the filter vector matching the desired signal can be determined.  $\mathbf{p}_0^{(1)}$  is calculated as follows. We first define  $\mathbf{v}_\pi = \mathbf{h}_{10} \mathbf{p}_1^{(1)} / \|\mathbf{h}_{10} \mathbf{p}_1^{(1)}\|$ , then  $\mathbf{p}_0^{(1)} = [\mathbf{v}_0^{(1)} - \mathbf{v}_\pi^H \mathbf{v}_0^{(1)} \mathbf{v}_\pi] / \|\mathbf{v}_0^{(1)} - \mathbf{v}_\pi^H \mathbf{v}_0^{(1)} \mathbf{v}_\pi\|$  is obtained. PUE can adopt  $\mathbf{f}_{0,M}^{(1)} = \mathbf{h}_0 \mathbf{p}_0^{(1)} / \|\mathbf{h}_0 \mathbf{p}_0^{(1)}\|$  as the receive filter. For space limit, we do not show the post-processed signal at PUE which can be referred to the derivations in the previous subsections.

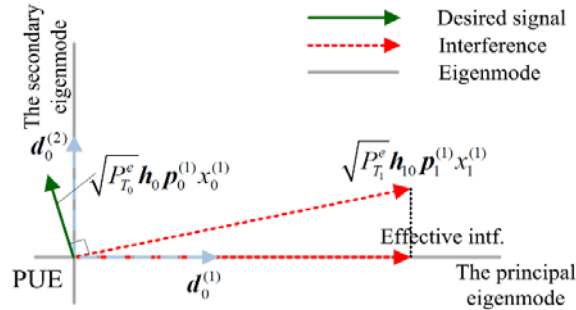


Fig. 6. An illustration of SD-ZFBF.

## 6. GENERALIZED DESIGN OF SDIG/TAICHI

### 6.1 Generalized Number of PBSs and PUEs

We now discuss the generalization of the number of PBSs deployed in the coverage of a macro-cell and the number of PUEs served by each PBS. In a hybrid cellular network

consisting of an MBS and multiple PBSs, each PBS schedules a PUE in a slot. All PBSs are within the coverage of the MBS. The CCI within the picocell can be avoided by allocating different resource blocks to the PUEs. We can also exploit spatial resource by employing proper precoders at the PBS so that concurrent transmissions to the PUEs are orthogonal to each other, hence eliminating CCI. However, in this case, the achievable number of orthogonal downlink transmissions is restricted by the antennas at the PBS and PUE. As mentioned above, PBSs are installed by the network operator. Inter-picocell interference could therefore be effectively avoided by the operator's planned deployment or resource allocation. In summary, with an appropriate system design, the proposed methods can be applied to the system with multiple PBSs and PUEs.

## 6.2 Generalized Number of MUEs

In the previous design, we assume that MBS sends one data stream to a MUE, *i.e.*, PUE is affected by only one disturbance. When there are multiple MUEs, multiple interferences may influence the PUE. In such a case, PBS can apply either IS directly to each interference, or IS and ZF reception to the aggregated effect of the interferences. The details can be found in [17, 18]. As for the interference between multiple MUEs, various multi-user downlink transmission schemes [19] can be employed, which is beyond the scope of this paper.

## 6.3 Design of SDIG/Taichi Under Imperfect CSI

So far, we have presented various IS implementations under instantaneous and perfect CSI, which is difficult to be obtained in practice, especially for fast varying channels. Therefore, exploiting statistical CSI (S-CSI) instead of instantaneous CSI (I-CSI) would be easier and cost-effective. Although S-CSI is somewhat more realistic than I-CSI, its inaccuracy may incur some performance loss compared to the schemes based on I-CSI. Moreover, the I-CSI-based designs and the results therein could still provide some theoretical conclusions.

There are several causes of partial CSI (or CSI error), including estimation error, CSI quantization, *etc.* The channel matrix can be modeled to account for CSI error as [20]:

$$\hat{\mathbf{H}} = \varepsilon \mathbf{H} + \sqrt{1 - \varepsilon^2} \mathbf{E} \quad (20)$$

where  $\mathbf{H}$  and  $\hat{\mathbf{H}}$  denote accurate and inaccurate channel matrices, respectively. Coefficient  $\varepsilon \in (0, 1]$  indicates the degree of CSI imperfection and  $\varepsilon = 1$  means perfect CSI. Matrix  $\mathbf{E}$  is an  $N_R \times N_T$  diagonal complex Gaussian matrix with zero mean and unit variance where  $N_R$  and  $N_T$  are the numbers of antennas equipped with the receiver and transmitter of a MIMO link. As shown in [21],  $\varepsilon$  can be used to indicate the impact of several factors on CSI, and hence is a function of the length of training sequence, SNR and Doppler frequency shift.

To improve the robustness of the proposed method to the abovementioned imperfect CSI, one can devise an iterative method based on either minimum mean-square error (MMSE) [22] or maximum signal-to-interference-plus-noise ratio (SINR) [22]. By exploiting the reciprocity/duality of wireless networks, a Max-SINR algorithm was proposed in [23] to obtain receive filters and precoding vectors so as to maximize SINR at the Rx's.

Since the design of SDIG/Taichi under S-CSI and imperfect CSI is beyond our scope, they are not elaborated in this paper. However, these can be matters of our future inquiry.

### 7. SIMULATION RESULTS

We now evaluate the proposed SDIG/Taichi using MATLAB simulation. The simulation parameters are given in Table 1 [16, 18].

In what follows, we will first set  $N_{T_0}=N_{R_0}=N_{T_1}=2$  in the simulation of Figs. 7-9. Then, we evaluate the performance of the proposed methods under more general antenna configurations (see in Fig. 10). Since  $N_{R_1}$  only affects the SE of MUE, we study the influence of this parameter to the system's SE in Fig. 11. According to the parameter settings in Table 1, since  $L_0$  and  $L_{10}$  are dependent on the system topology, *i.e.*, the locations of MBS, PBS, MUE and PUE, we can obtain that  $P_e$  ranges from  $-89$  dBm to  $23$  dBm, whereas  $P_{T_0}^e$  varies between  $\eta = P_{T_1}^e/P_{T_0}^e$  to represent the relative strength of interference to the desired signal perceived by PUE. Then, based on the above parameter settings, we can derive  $\eta \in [-135, 123]$  dB. Note, however, that we obtained this result for extreme boundary situations, so its range is too wide to be useful. In practice, a PBS should not be deployed close to MBS and mobile users may select an access point based on the strength of reference signals from multiple access points. Based on this practice, we set  $\eta \in [0.01, 10]$  in our simulation [18]. In evaluation, we also define a factor  $\zeta = \cos\theta$  to indicate the correlation between the spatial have  $\zeta \in [0, 1]$ . We define signal-to-noise ratio (SNR) as  $\text{SNR} = 10 \log_{10}(P_{T_0}/\sigma)$  dB in features of the interference and the principal eigenmode of  $\mathbf{h}_0$ . Since  $\theta \in [0, \pi/2]$ , we can have  $\zeta \in [0, 1]$ . We define signal-to-noise ratio (SNR) as  $\text{SNR} = 10 \log_{10}(P_{T_0}/\sigma_n^2)$  dB in the simulation. Moreover, in the evaluation, when the IM is unavailable, *i.e.*, the power cost for IS exceeds the budget at PBS, non-IM (*i.e.*, PUE employs MF in reception) is adopted. Since IA is realized by the interfering Tx, yielding some SE loss of the interfering transmission pair, whereas no SE loss is incurred by IA to the interfered transmission pair, we do not simulate SD-IA in the evaluation of PUE's SE performance.

**Table 1. Parameter settings.**

| Parameter                  | Value  |
|----------------------------|--|
| The radius of pico-cell    | 300 m  |
| The radius of macro-cell   | 3000 m   |
| Transmit power of MBS      | 46 dBm   |
| Transmit power of PBS      | 23 dBm   |
| Path loss from MBS to a UE | $L_{(c)} = 128.1 + 37.6 \log_{10}[\rho_{(c)}/10^3]$ dB |
| Path loss from PBS to a UE | $L_{(c)} = 38 + 30 \log_{10}[\rho_{(c)}]$ dB           |
| Range of $P_{T_1}^e$       | $[-89, 23]$ dBm  |
| Range of $P_{T_0}^e$       | $[-100, 46]$ dBm                                       |

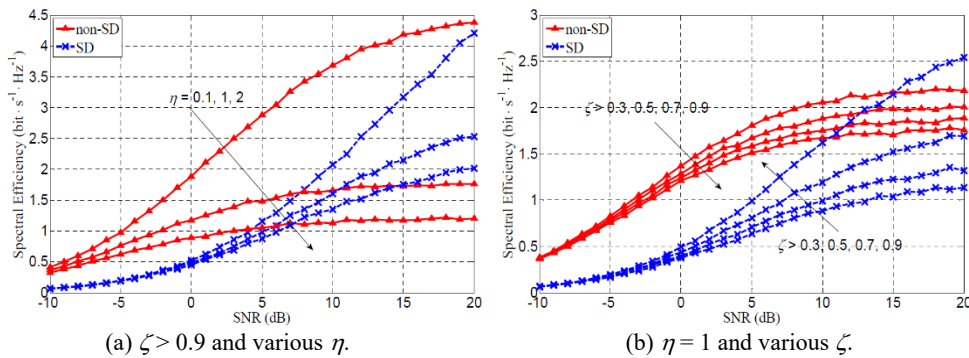


Fig. 7. Spectral efficiency of PUE vs. SNR with and without SD.

Fig. 7 plots the variation of PUE's SE with SNR under various  $\zeta$  and  $\eta$ . The detailed signal processing can be found in Section 4. As the figure shows, large  $\zeta$  indicates strong effective interference imposed on PUE, yielding the PUE's SE of SD to be superior to that of non-SD. Under fixed  $\zeta$ , both SD and non-SD output decreased SE as  $\eta$  grows. This is because the interference becomes strong with an increase of  $\eta$ , incurring low received signal-to-interference-plus-noise ratio (SINR) at PUE. From Fig. 7 (b) we can see that given fixed  $\eta$ , PUE's SE with SD grows as  $\zeta$  increases whereas for non-SD, PUE's SE decreases. This is because given the same interference, its projection on the principal and secondary eigenmodes of  $\mathbf{h}_0$  increases and decreases, respectively, as  $\zeta$  grows, incurring degradation and improvement of PUE's SE with non-SD and SD, respectively.

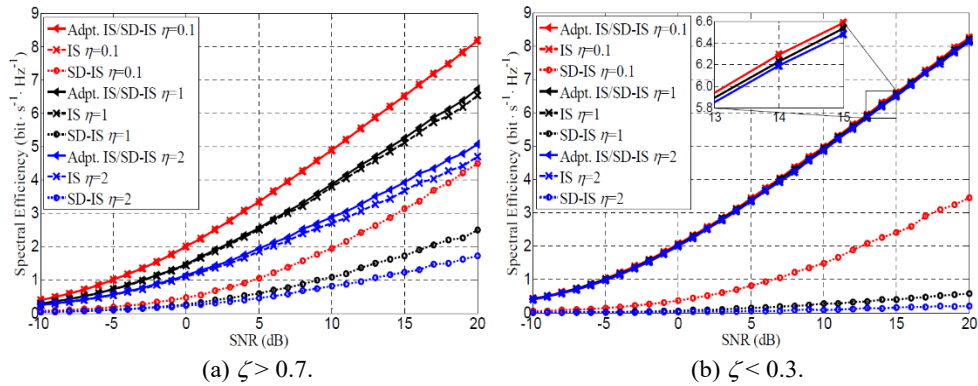


Fig. 8. Spectral efficiency of PUE vs. SNR under  $\zeta > 0.7$ ,  $\zeta < 0.3$  and different  $\eta$  with IS (without SD), SD-IS and their adaptation.

Fig. 8 shows the PUE's SE of IS, SD-IS and their adaptation. As the figures show, the adaptive selection of IS and SD-IS, *i.e.*, Adpt. SD/SD-IS can provide the best SE. Given fixed  $\eta$ , PUE's SE with SD-IS under a large  $\zeta$  exceeds that under low  $\zeta$ . This is because under large  $\zeta$ , IS can adjust the disturbance to the principal eigenmode with less power overhead, while steering interference to the secondary mode costs more power. The detailed analysis can be found in the discussion about Fig. 7. As  $\eta$  increases, PUE's SE reduces. This is due to the fact that given a large  $\eta$ , the interference perceived by PUE becomes stronger. In addition, the probability that PBS's power is insufficient for IS increases, incurring an increase of IS's infeasible probability. The gap between IS and SD-IS under identical parameter setting increases as  $\eta$  grows, indicating that SD-IS becomes more preferable as  $\eta$  increases. As Fig. 8 (b) shows, SE of IS overlaps with that of Adpt. IS/SD-IS. This is because when  $\zeta < 0.3$ , the power cost and performance loss of SD-IS are more while its benefit is less, yielding IS's SE to outperform SD-IS's, and hence IS is adopted with high probability.

Fig. 9 plots PUE's SE of ZF (without SD), SD-ZF and their adaptation. As the figure shows, SE performance is independent of  $\eta$ . This is because the ZF filter is determined only by the spatial feature of the interference perceived by PUE. As aforementioned, the necessity of SD is dependent on the spatial correlation between the disturbance and the principal eigenmode occupied by the desired transmission. Given large  $\zeta$  (Fig. 9 (a)), SD-ZF outputs higher PUE's SE than that under low  $\zeta$  (Fig. 9 (b)).

Moreover, since the design of ZF filter is highly dependent on the value of  $\zeta$ , SE curves of ZF and Adpt. ZF/SD-ZF in Fig. 9 (b) exceed those in subplot (a).

Fig. 10 plots PUE's SE of IS, SD-IS and their adaptation under  $\zeta > 0.7$ ,  $\eta = 2$  and various antenna configurations. For clarity, we use a general form  $[N_{T_0} N_{R_0} N_{T_1}]$  to express

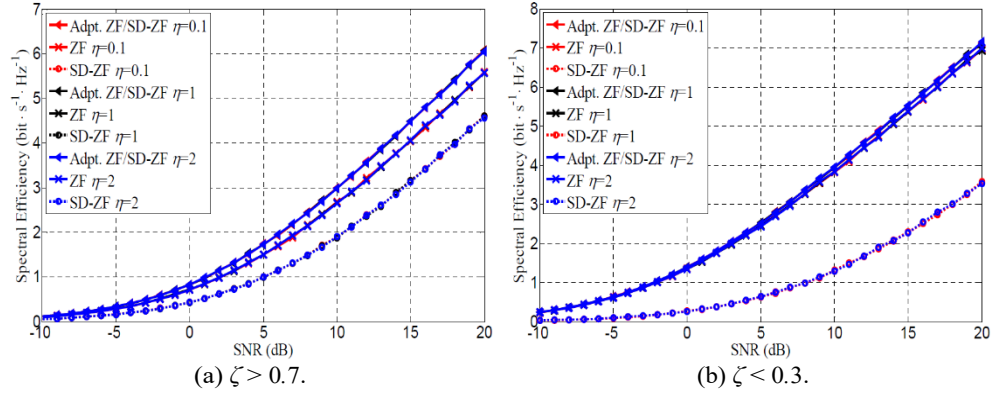


Fig. 9. Spectral efficiency of PUE vs. SNR under  $\zeta > 0.7$ ,  $\zeta < 0.3$  and different  $\eta$  with ZF (without SD) and SD-ZF and their adaptation.

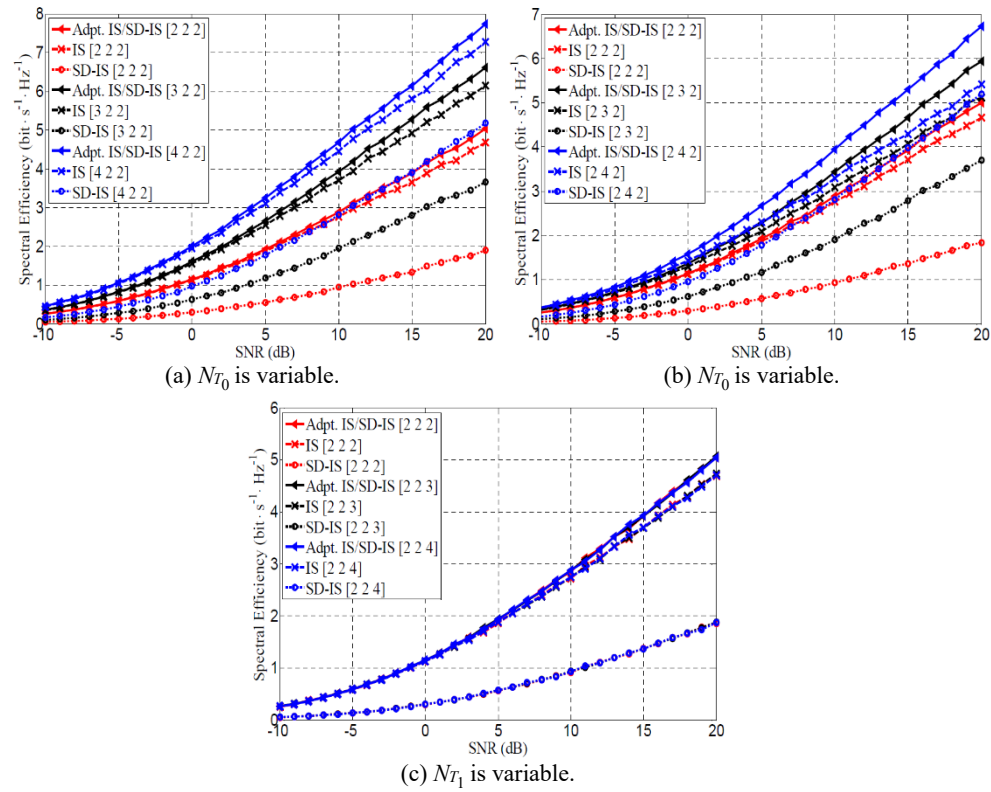


Fig. 10. Spectral efficiency of PUE vs. SNR under  $\zeta > 0.7$ ,  $\eta = 2$  and various antennas settings.

the antenna configuration. As the figure shows, Adpt. IS/SD-IS outputs the best SE, which implies that SD-IS should be properly adopted due to its superior performance to IS under some transmission conditions. Fig. 10 (a) shows the influence of  $N_{T_0}$  on PUE's SE. As can be seen, SE of all three methods grows as  $N_{T_0}$  increases. This is because large  $N_{T_0}$  brings more transmit diversity gain, yielding an increase of PUE's SE. As Fig. 10 (b) shows, PUE's SE increases as  $N_{R_0}$  grows. This is due to the fact that more receive diversity gain is introduced by a large  $N_{R_0}$ . In Fig. 10 (c), PUE's SE is independent of  $N_{T_1}$ . This is because the interference from MBS to PUE is random, this property is irrelevant to the value of  $N_{T_1}$ .

Fig. 11 shows the system's SE of SD-IA, SD-ZF, SD-IS, SD-ZFBBF and their adaptation (denoted by Adpt. X/SD-X) under  $N_{T_0}=N_{R_0}=N_{T_1}=N_{R_1}=2$ . Adpt. X/SD-X is shown to output the highest SE. From the system's point of view, given a small  $\eta$  (see in Fig. 11 (a)), SD-IS is the best among the four candidate methods, whereas SD-IA and SD-ZF rank the second and third, respectively. SD-ZFBBF performs the worst. Provided with a large  $\eta$ , SD-IA is most preferable, then come SD-ZF and SD-IS. SD-ZFBBF still yields the lowest SE.

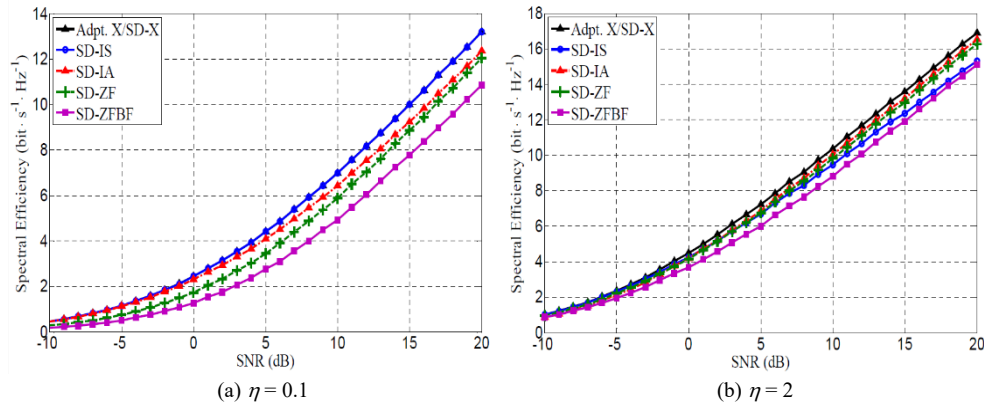


Fig. 11. System' SE vs. SNR with various IM schemes.

## 8. CONCLUDING REMARKS

In this paper, we proposed and evaluated a novel interference management technique, called *signal dodging and interference guiding* (SDIG) or *Taichi*. We first adjust the data transmission from the principal eigenmode to the secondary one, so that the influence of interference to the desired transmission can be partially avoided. Then, by combining with existing (active) IM method, the disturbance can be further moved away from the desired signal. This is similar to the idea of Taichi. Our in-depth simulation has shown that with appropriate use of SD and selection of IG methods, both the interfered transmission pair's and the system's SE can be significantly improved.

## ACKNOWLEDGMENT

This work was supported in part by the Project of Cyber Security Establishment with Inter University Cooperation; the Secom Science and Technology Foundation.

## REFERENCES

1. Qualcomm, "5G-Vision for the next generation of connectivity," 2015.
2. M. Y. Arslan, J. Yoon, K. Sundaresan, *et al.*, "FERMI: A femtocell resource management system for interference mitigation in OFDMA networks," in *Proceedings of International Conference on Mobile Computing and Networking*, 2011, pp. 25-36.
3. A. Mukherjee, D. De, and P. Deb, "Interference management in macro-femtocell and micro-femtocell cluster-based long-term evaluation-advanced green mobile network," *IET Communications*, Vol. 10, 2016, pp. 468-478.
4. W. L. Shen, K. C.-J. Lin, S. Gollakota, and M.-S. Chen, "Rate adaptation for 802.11 multiuser MIMO networks," *IEEE Transactions on Mobile Computing*, Vol. 13, 2014, pp. 35-47.
5. T. Yoo and A. Goldsmith, "On the optimality of multiantenna broadcast scheduling using zero-forcing beamforming," *IEEE Journal on Selected Areas in Communications*, Vol. 24, 2006, pp. 528-541.
6. S. A. Jafar, "Interference alignment – A new look at signal dimensions in a communication network," *Foundations and Trends in Communications and Information Theory*, Vol. 7, 2011, pp. 1-134.
7. X. Rao, L. Ruan, and V. K. N. Lau, "Limited feedback design for interference alignment on MIMO interference networks with heterogeneous path loss and spatial correlations," *IEEE Transactions on Signal Processing*, Vol. 61, 2013, pp. 2598-2607.
8. Z. Li, J. Chen, L. Zhen, *et al.*, "Coordinated multi-point transmissions based on interference alignment and neutralization," *IEEE Transactions on Wireless Communications*, Vol. 18, 2019, pp. 3347-3365.
9. Z. Li, Y. Liu, Kang G. Shin, J. Liu, and Z. Yan, "Interference steering to manage interference in IoT," *IEEE Internet of Things Journal*, Vol. 6, 2019, p. 1.
10. V. R. Cadambe and S. A. Jafar, "Interference alignment and degrees of freedom of the  $K$  user interference channel," *IEEE Transactions on Information Theory*, Vol. 54, 2008, pp. 3425-3441.
11. T. Liu and C. Yang, "On the feasibility of linear interference alignment for MIMO interference broadcast channels with constant coefficients," *IEEE Transactions on Signal Processing*, Vol. 61, 2013, pp. 2178-2191.
12. S. A. Jafar and M. J. Fakhreddin, "Degrees of freedom for the MIMO interference channel," *IEEE Transactions on Information Theory*, Vol. 53, 2007, pp. 2637-2642.
13. Z. Li, K. G. Shin, and L. Zhen, "When and how much to neutralize interference?" in *Proceedings of IEEE International Conference on Computer Communications*, 2017, pp. 1-9.
14. Y. Mehmood, C. Görg, and A. Timm-Giel, "A radio resource sharing scheme for IoT/M2M communication in LTE-A downlink," in *Proceedings of IEEE International Conference on Communications*, 2016, pp. 296-301.
15. D. Lee, H. Seo, B. Clerckx, *et al.*, "Coordinated multipoint transmission and reception in LTE-advanced: Deployment scenarios and operational challenges," *IEEE Communications Magazine*, Vol. 50, 2012, pp. 148-155.
16. 3GPP TR 36.931 Release 14, "LTE; Evolved Universal Terrestrial Radio Access (EUTRA); Radio Frequency (RF) requirements for LTE Pico Node B," 2017.

17. Z. Li, Y. Liu, K. G. Shin, *et al.*, "Design and adaptation of multi-interference steering," *IEEE Transactions on Wireless Communications*, Vol. 18, 2019, pp. 3329-3346.
18. Z. Li, F. Guo, C. Shu, K. G. Shin, *et al.*, "Dynamic interference steering in heterogeneous cellular networks," *IEEE Access*, Vol. 6, 2018, pp. 28552-28562.
19. L.-U. Choi and R. D. Murch, "A transmit preprocessing technique for multiuser MIMO systems using a decomposition approach," *IEEE Transactions on Wireless Communications*, Vol. 3, 2014, pp. 20-24.
20. H. A. Suraweera, P. J. Smith, and M. Shafi, "Capacity limits and performance analysis of cognitive radio with imperfect channel knowledge," *IEEE Transactions on Vehicular Technology*, Vol. 59, 2010, pp. 1811-1822.
21. K. S. Ahn and R. W. Heath, "Performance analysis of maximum ratio combining with imperfect channel estimation in the presence of cochannel interferences," *IEEE Transactions on Wireless Communications*, Vol. 8, 2009, pp. 1080-1085.
22. G. C. Alexandropoulos, P. Ferrand, and C. B. Papadias, "On the robustness of coordinated beamforming to uncoordinated interference and CSI uncertainty," in *Proceedings of IEEE Wireless Communications and Networking Conference*, 2017, pp. 1-6.
23. K. Gomadam, V. R. Cadambe, and S. A. Jafar, "A distributed numerical approach to interference alignment and applications to wireless interference networks," *IEEE Transactions on Information Theory*, Vol. 57, 2011, pp. 3309-3322.



**Liyuan Xiao** received the Ph.D. degree in Communication and Information Systems from Xidian University, Xi'an, China, in 2011. She is currently doing postdoctoral research in the School of Information Science and Technology, Northwest University. She has published over 30 technical papers at journals and conferences. Her research interests include resource management, interference management, wireless communication and 5G communication systems.



**Zhao Li** received the BS degree in Telecommunications Engineering, the MS and Ph.D. degrees in Communication and Information Systems from Xidian University, Xi'an, China, in 2003, 2006, and 2010, respectively. He is currently an Associate Professor in the School of Cyber Engineering, Xidian University. He worked as a visiting scholar and then research scientist in the Real-Time Computing Laboratory in the Department of Electrical Engineering and Computer Science, The University of Michigan, during 2013-2015. He has published over 40 technical papers at premium international journals and conferences, like IEEE IoT Journal, IEEE TWC, IEEE INFOCOM, Computer Communications, and so on. His research interests include wireless communication, 5G communication systems, resource allocation, interference management, IoT and physical layer security.



**Lu Zhen** is currently a Master student in the School of Telecommunications Engineering at Xidian University. Her research interests include wireless communication, resource allocation, interference management and security communication.



**Jia Liu** received the Ph.D. degree from the School of Systems Information Science, Future University Hakodate, Japan, in 2016. He is currently an Assistant Professor in the Center for Cybersecurity Research and Development, National Institute of Informatics, Japan. His research interests include mobile ad hoc networks, 5G communication systems, D2D communications, IoT, physical layer security, cyber security, *etc.* He has published over 20 technical papers at premium international journals and conferences, like IEEE TWC, IEEE TVT, IEEE INFOCOM, Computer Networks, and so on. He is the winner of 2016 IEEE Sapporo Section Encouragement Award and the Best Paper Award of NaNA 2017.



**Yang Xu** received the B.E. degree from the School of Telecommunications Engineering and the Ph.D. degree from the Department of Communication and Information Systems, Xidian University, Xi'an, China, in 2006 and 2014, respectively, where she is currently a lecturer with the School of Economics and Management, The State Key Laboratory of Integrated Services Network. She has published about 30 papers at premium international journals, including IEEE TVT, IEEE TWC, and Computer Networks. She has published in conferences including IEEE ICC and IEEE WCNC. Her current research interests include physical layer security, block-chain, routing protocol design and network performance evaluation.